Chemical and Electrochemical Properties of [Cp*Rh] Complexes Supported by a Hybrid Phosphine-Imine Ligand

Julie A. Hopkins, Davide Lionetti, Victor W. Day, and James D. Blakemore*

Department of Chemistry, University of Kansas, 1251 Wescoe Hall Drive, Lawrence, Kansas 66045, United States

Supporting Information Placeholder

ABSTRACT: A series of [Cp*Rh] complexes (Cp* = η^5-pentamethylcyclopentadienyl) bearing the κ^2-[*P,N*]-8-(diphenylphosphino)quinoline (PQN) ligand have been prepared and characterized. Chemical or electrochemical reduction of the rhodium(III) form generates an isolable rhodium(I) complex; this rhodium(I) complex reacts with a range of organic acids to yield a rhodium(III) hydride bearing [Cp*] in the η^5 mode and [PQN] in the expected κ^2 mode. Solid state structures of these three compounds from X-ray diffraction studies reveal only small changes in the intraligand bond distances across the series, suggesting the redox events associated with interconversion of these compounds are primarily metal-centered. Cyclic voltammetry data show that the rhodium(III) chloride complex undergoes a two-electron reduction at –1.19 V vs. ferrocenium/ferrocene, whereas the analogous solvento rhodium(III) acetonitrile complex undergoes two, sequential one-electron reductions. The rhodium(III) hydride undergoes an irreversible, ligand-centered reduction near –1.75 V vs. ferrocenium/ferrocene. Carrying out this reduction alone or in the presence of added of triethylammonium as a source of protons results in only modest yields of H_2, as shown by bulk electrolyses and chemical reduction experiments. These results are discussed in the context of recent work with [Cp*Rh] complexes bearing more symmetric 2,2′-bipyridyl and diphosphine ligands.

INTRODUCTION

Effective management of both protons (H^+) and reducing equivalents (e^-) can maximize efficiency in small-molecule activation processes, such as evolution of dihydrogen (H_2) and reduction of carbon dioxide (CO_2) to more useful chemicals.[1] Consequently, the study of metal complexes that can serve as catalysts or model compounds in such transformations is an area of robust activity within the field of energy science. Knowledge of the reactivity that metal complexes undergo when reduced and/or protonated is of especially high interest, since these reactions are nearly always involved in reductive, fuel-forming catalysis.

Reduction and protonation events are often metal-centered, and lead to formation of metal hydride complexes.[2] On the other hand, ligands may also be "non-innocent," and thus become intimately involved in reduction and protonation chemistry.[3] Understanding of these events can enable tuning of catalysis, and/or transfer of multiple H^+/e^- equivalents with modest energy penalties.[4] However, it remains difficult to predict and/or control transfer of electrons and protons to metal complexes. In systems that contain non-innocent ligands, understanding the nature of catalysis or the catalytic mechanism is especially challenging, as the locus of reduction or protonation may be metal- or ligand-centered.[5]

Recently, we have been working to understand reduction and protonation reactivity in a model family of organometallic rhodium complexes that can serve, in some cases, to couple H^+/e^- equivalents as molecular electrocatalysts for H_2 evolution. The complexes of interest are supported by the pentamethylcyclopentadienyl (Cp*) ligand, as well as an additional bidentate ligand; work to date has examined the properties of symmetric, bidentate chelates containing nitrogen or phosphorus donors (Chart 1, ^{R}**A** and **B**). The parent catalyst was reported by Grätzel and Kölle in 1987 to be an electrocatalyst for H_2 evolution, and bears the common 2,2′-bipyridyl ligand (^{H}bpy).[6] Although several studies have examined this catalyst system, the full mechanism that guides H_2 generation has not been reported.[7] Original proposals involved reduction to form a rhodium(I) complex followed by two H^+ transfer events; the first protonation was expected to generate a Rh^{III}–hydride species, which would then be protonolyzed by the second H^+ equivalent to generate H_2. This system can also catalyze reactions involving transfer of [H^-] to other acceptor molecules, like NAD^+.[8] However, the putative [Cp*Rh–H] intermediates have only been observed under stringent conditions,[9] and have not yet been fully characterized.

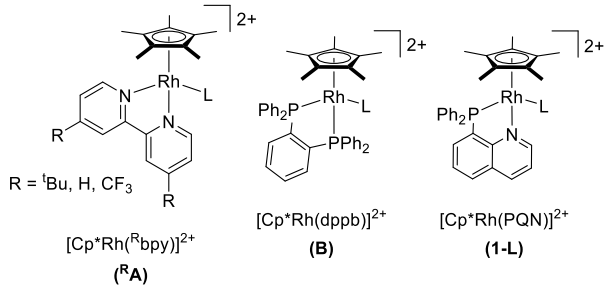

Chart 1. Half-sandwich Rh complexes supported by N- and P-containing bidentate ligands.

More recently, parallel reports from our group[10] and Miller's group[11] have shown that protonation of the isolable Rh(I) complex Cp*Rh(^{H}bpy) can result in clean transfer of the incoming H^+ equivalent to the [Cp*] ring. Spectroscopic (proton nuclear magnetic resonance, ^{1}H NMR) and structural (X-ray diffraction, XRD) studies reveal generation of an *endo*-η^4-pentamethylcyclopentadiene ([Cp*H]) species

containing a formally Rh(I) center stabilized by π-backbonding interactions with the nascent diolefin ligand.[12] Such reactivity, in which a cyclopentadienyl ligand apparently acts as a pendant base, has been discussed and experimentally implicated in catalytic processes with a variety of organometallic species.[13,14,15] Because [Cp*] is ubiquitous in catalysis but is typically considered to be an innocent ancillary ligand, new knowledge related to the phenomenon of reversible [Cp*] protonation could open new opportunities in catalyst design.

Building on our initial findings with half-sandwich complexes, we have found that [Cp*H] rhodium complexes can be supported by a variety of disubstituted bipyridyl ligands, independent of their electron-withdrawing or electron-donating nature. Complexes bearing ^{t}Bu– (^{tBu}bpy) or CF_3– (^{CF3}bpy) substituents are catalytically active for H_2 evolution, and generate [Cp*H] species *in situ* upon treatment of reduced precursors with appropriate H^+ sources.[16] Analogous behavior has also been observed for a complex supported by 1,10-phenanthroline (phen).[12]

Moreover, we have found that reduction of these [Cp*H] complexes by one additional e^- enables access to a new catalytic cycle leading to H_2 formation. Specifically, reduction of [Cp*H] complexes supported by ^{R}bpy ligands (R = H, CF_3) results in generation of unstable complexes that undergo net transfer of a hydrogen atom (H•), yielding the corresponding rhodium(I) complexes and H_2. In fact, electrochemical experiments on complex ^{CF3}**A** (Chart 1) indicate that this new catalytic pathway is responsible for the majority of the catalytic current enhancement, whereas the enhancement of the current corresponding to the rhodium(III/I) couple is less significant.[16] Based on the electrochemical potentials involved, and by comparison to other complexes, reduction of these [Cp*H] complexes is proposed to be centered on the ^{R}bpy ligand, whose redox non-innocence is well documented.[17] However, evidence is not yet available to distinguish between the possible homolytic (net release of H•) and heterolytic (protonolysis by an exogenous H^+ source) pathways that lead to H_2 evolution.[18]

Because of the likely involvement of transient hydride complexes in this chemistry, we have recently been investigating the synthesis and reactivity properties of [Cp*Rh] monohydrides. Prior work with such compounds,[19] and notable analogues,[20] suggested to us that phosphine ligands would provoke formation of the Rh–H interaction. Indeed, we have recently shown that the 1,2-bis(diphenylphosphino)benzene ligand (dppb) drives formation of a rhodium(III) complex (**B**, Chart 1) that can be readily reduced and cleanly protonated to generate a stable rhodium(III)–hydride.[21] Unlike the tautomeric [Cp*H] species observed in ^{R}bpy-ligated systems, this [Rh–H] complex is remarkably resistant to further reactivity; the Rh–H bond does not undergo protonolysis even in the presence of strong acids in organic solvents. Furthermore, this hydride undergoes metal-centered reduction at a quite negative potential ($E_{1/2}(Rh^{III}/Rh^{II})$ = –2.25 vs. the ferrocenium/ferrocene couple, subsequently noted as $Fc^{+/0}$), precluding electrocatalytic studies. Thus, the ability to access [Cp*H]-type compounds appears essential for catalysis with [Cp*Rh] systems. However, only [Cp*Rh] complexes bearing diimine and diphosphine ligands have been explored so far in this chemistry. Thus, an opportunity lies in probing the reactivity profile engendered by less symmetric, hybrid ligands that could provide the electronic characteristics engendered through inclusion of a single phosphine donor and a single imine donor.

Here, we report synthesis, characterization, and reactivity studies of [Cp*Rh] complexes supported by such a hybrid ligand, 8-(diphenylphosphino)quinoline (PQN). PQN presents a triarylphosphine donor and an imine donor with appropriate disposition for formation of an attractive five-membered metallacycle, complementing our prior work with dppb and 4,4′-disubstituted-2,2′-bipyridyls. The coordination chemistry of PQN ligands has been studied with several transition metals, including Pd,[22,23,24] Cu,[25] Ni,[26] Au,[27] Ru,[28] Zn,[29] Ir,[30] and Pt[23]; however, only two short reports regarding Rh complexes are available,[23,31] and no half-sandwich complexes have been investigated. We find that the PQN ligand engenders properties on [Cp*Rh] that are intermediate between those of systems supported by ^{R}bpy ligands and by the dppb scaffold: while the potential of the rhodium(III/I) couple of the [Cp*Rh(PQN)Cl]$^+$ (**1-Cl**) complex is more similar to that of the corresponding ^{R}bpy systems, protonation of the rhodium(I) complex **2** yields a rhodium(III)–hydride species (**3**), similarly to the dppb-supported complex. Importantly, we find that the PQN-supported hydride undergoes ligand-centered reduction, unlike the metal-centered reduction observed for the dppb-supported hydride. Based on chemical and electrochemical work carried out in the presence of acid, we find that **3** can only slowly generate H_2 in the presence of acid, and that electrochemical reduction of **3** leads to low yields of H_2 accompanying formation of multiple metal-containing products. Taken together, we conclude that use of the hybrid ligand PQN to enable formation of a hydride does not favor robust H_2 evolution, further underscoring the unique profile accessed by analogous [Cp*H] complexes.

RESULTS

Synthesis and Electrochemical Characterization of [Cp*Rh] Complexes. The dimeric $[Cp^*RhCl_2]_2$ complex[32] is a useful precursor that can be utilized to prepare [Cp*Rh] complexes containing chelating bidentate ligands in a straightforward manner.[33] For the present [*P,N*] system, 2 equiv. of AgOTf were added to $[Cp^*RhCl_2]_2$, followed by 2.05 equiv. of free PQN (synthesized by the methods of Haftendorn[34]and Metzger[35]) to give the orange rhodium(III) complex **1-Cl** (Scheme 1).

Scheme 1. Preparation of [Cp*Rh] complexes.

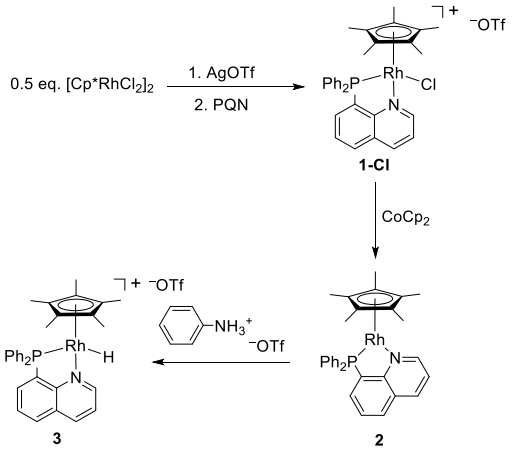

Characterization of this material by proton nuclear magnetic resonance (^{1}H NMR) reveals a signal at 1.54 ppm integrating to 15H that displays coupling to the NMR-active phosphorus nucleus ($^4J_{H,P} \approx 3.8$ Hz), and can therefore be assigned to the equivalent [Cp*] protons. (See SI, Figure S4). In addition, a doublet ($^1J_{P,Rh} \approx 143.8$ Hz) was observed at 47.90 ppm in the $^{31}P\{^1H\}$ NMR spectrum of **1-Cl**, corresponding to the Rh-bound phosphorus atom. Vapor diffusion of diethyl ether (Et_2O) into acetonitrile (CH_3CN) yielded orange crystals of **1-Cl** suitable for X-ray diffraction (XRD) studies. The resulting solid-state structure reveals the geometry of the formally Rh(III) metal center in **1-Cl** as *pseudo*-octahedral (Figure 1). The first coordination sphere around the metal contains the κ^2-[*P,N*]-PQN scaffold, a single bound chloride anion, and the [η^5-Cp*] ligand. The angle between the plane of the [Cp*]

ligand the plane of the bidentate ligand (the plane defined by the Rh, N and P atoms) is ~81°, which is substantially larger than the analogous angle in the [Cp*Rh(bpy)Cl]$^+$ system (~59°).[36] This difference in complexation angle suggests that the steric bulk of the PQN ligand effects the geometry within the [Cp*Rh] and the bidentate framework.

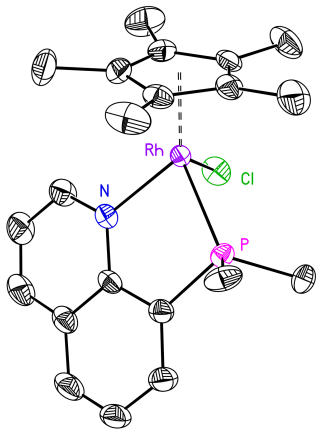

Figure 1. Solid-state structure of **1** (XRD); triflate counteranion and hydrogen atoms omitted for clarity. Phenyl groups truncated for clarity. Thermal ellipsoids shown at the 50% probability level.

Electrochemical studies were conducted to investigate the redox behavior engendered by the PQN ligand. Previously studied [Cp*Rh] systems bearing various 2,2′-bipyridyl (bpy) derivatives[6,16] undergo a single 2e$^-$ reduction from Rh(III) to Rh(I) via an ECE′-type mechanism[37] (E = electron transfer, C = chemical reaction) in which the monodentate ligand of the Rh(III) species is lost upon reduction. The cyclic voltammogram (CV) of **1-Cl** exhibits a similar appearance, with a first reduction event at –1.19 V vs. $Fc^{+/0}$ (Figure 2), which appears to be a quasi-reversible, 2e$^-$ process corresponding to reduction of Rh(III) to Rh(I) (*vide infra*). This behavior indicates that **1-Cl** undergoes a similar ECE′ process in relation to the previously reported bpy complexes: initial 1e$^-$ reduction of the chloride-bound Rh(III) species **1-Cl** generates a transient 19-electron complex (E). Loss of the Cl$^-$ ligand then results in formation of a 17-electron species (C); the rhodium(II/I) reduction potential of this transient intermediate is very near to the rhodium(III/II) potential of **1-Cl**, resulting in immediate transfer of a second electron (E′).

During the ECE′ sequence, bpy-supported [Cp*Rh] complexes undergo a geometric rearrangement to a *pseudo*-square planar geometry, which improves overlap between empty π-symmetry orbitals on the bidentate framework and metal d orbitals, thereby activating π-backbonding to the bidentate ligand. These bpy complexes engage in π-backbonding by extensive delocalization of electron density into the ligand LUMO at the formally rhodium(I) oxidation state. As a result, the bpy bound to [Cp*Rh] appears to have significant reduced character as judged by crystallography,[38] as well as spectroscopic and theoretical methods.[17,39,40] In the case of the present system bearing [PQN], the bidentate ligand undergoes only a minor change in orientation upon reduction (vide infra), suggesting that its greater steric bulk (vs. bpy) effects its tendency to engage in π-backbonding.

Additionally, a third 1e$^-$ reduction is observed for **1-Cl** centered at –2.26 V vs. $Fc^{+/0}$; an analogous reduction event has been reported in [Cp*Rh] complexes supported by bpy and 1,10-phenanthroline (phen), albeit at more negative potentials.[40,41] We note here that the metal-free PQN ligand can be redox active itself, and undergoes a more negative reduction event at –2.46 V (see SI, Figure S54). Thus, the third reduction measured here cannot yet be reliably assigned as either ligand- or metal-centered. Further work with relevant model compounds could provide helpful comparisons in future work. However, we do note here that scan rate-dependent studies verify that all species present in the cyclic voltammetry of **1-Cl** are freely diffusing and soluble (Figure S41 and S42).

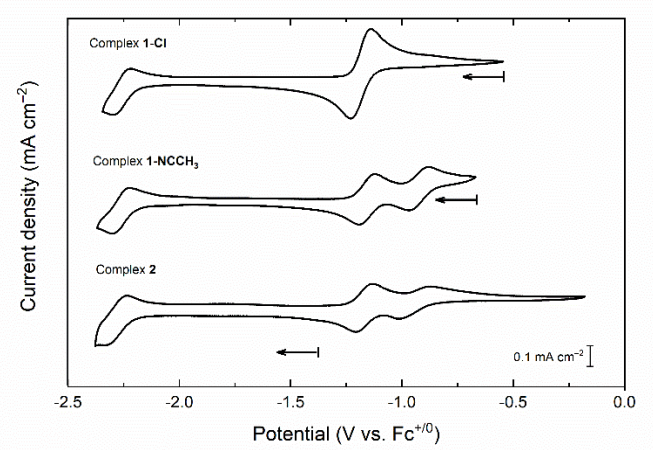

Figure 2. Cyclic voltammetry of **1-Cl** (upper), **1-NCCH$_3$** (middle), and **2** (lower). Electrolyte: 0.1 M $TBAPF_6$ in CH_3CN; Scan rate: 100 mV/s; Working electrode: highly oriented pyrolytic graphite (HOPG); [Rh] in each experiment was ca. 1 mM. Initial potentials (marked with the start line of each arrow): **1-Cl**, ca. –0.5 V ; **1-NCCH$_3$**, ca. –0.7 V; **2**, ca. –1.4 V.

Chloride is implicated to play a key role in the events governing the electrochemical reduction of **1-Cl**, because it serves as a ligand in the starting material and is lost upon the first one-electron reduction. To provide better support for assignment of this role for chloride, we turned to chemical preparation of the analogous acetonitrile-bound solvento species, **1-NCCH$_3$**. Specifically, 1 equiv. of **1-Cl** was treated with 1 equiv. of AgOTf in CH_3CN solvent. Filtration to remove the co-generated AgCl precipitate and removal of excess solvent *in vacuo* enabled isolation of the metastable solvento complex **1-NCCH$_3$**. Notably, the pure compound could be fully characterized by ^{1}H, ^{13}C{^{1}H}, ^{31}P{^{1}H}, and ^{19}F NMR, as well as ESI-MS (see SI, Figures S28-S31). However, satisfactory elemental analysis could not be obtained due to association of a slight excess of solvent with the otherwise clean, isolated material. Upon extended drying to fully remove CH_3CN, decomposition was encountered, likely driven by solvent loss. Similar observations have been made in prior synthetic work with solvento [Cp*Rh] and [Cp*Ir] complexes.[42]

In accord with the implicated role for chloride, the profile of cyclic voltammetry carried out with **1-NCCH$_3$** is distinct from that of **1-Cl**. Starting at positive potential, a negative-going scan reveals two sequential one-electron reduction events, in contrast to the single two-electron event measured for **1-Cl**. Specifically, we observe a first reduction of **1-NCCH$_3$** centered at –0.93 V, followed by a second reduction at –1.16 V. These events are quasi reversible, and correspond to the formal Rh(III/II) and Rh(II/I) couples, respectively. Both events are quasi-reversible, although the peak-to-peak separation (ΔE_p) for the first event (90 mV) is slightly greater than that of the second event (70 mV). These values are consistent with the expected loss of coordinated CH_3CN upon the first one-electron reduction (i.e., reduction results in generation of a transient 19e$^-$ Rh^{II} complex which undergoes loss of CH_3CN to

form a metastable 17e⁻ complex bearing only [Cp*] and [PQN]). This process is very similar to the reduction-induced loss of chloride implicated in the work with **1-Cl**. Finally, scan rate-dependent studies verify that all species present in the cyclic voltammetry of **1-NCCH$_3$** are freely diffusing and soluble (Figure S44).

Within this model, the reduction of **1-NCCH$_3$** via two, sequential one-electron reductions and reduction of **1-Cl** in the two-electron event discussed above should produce an identical, formally rhodium(I) product. Consistent with this notion, the third one-electron reduction event centered at –2.26 V measured with **1-Cl** is observed at a virtually identical potential in the voltammetry with **1-NCCH$_3$**. Thus, we conclude that the reduction product is identical in these two cases; this product would be formulated as Cp*Rh(PQN) (**2**), produced by loss of chloride from **1-Cl** and loss of CH_3CN from **1-NCCH$_3$**.

With these electrochemical data in hand, we targeted chemical isolation of the reduced species **2**. Addition of cobaltocene (Cp_2Co, E^o = –1.31 V vs. $Fc^{+/0}$,[43] 1.9 equiv.) to **1-Cl** in a thawing mixture of tetrahydrofuran (THF) and CH_3CN results in a rapid, significant darkening of the reaction solution; removal of volatiles *in vacuo* and extraction with hexane yielded a dark red-orange solid. The ^{1}H NMR spectrum of this material displays a signal at 1.98 ppm ($^4J_{H,P} \approx 1.2$ Hz) corresponding to the [Cp*] protons (see SI, Figure S12). In the $^{31}P\{^1H\}$ NMR spectrum, this material displays a doublet ($^1J_{P,Rh} \approx 246.3$ Hz) at 55.29 ppm; the downfield shift and substantial increase in coupling constant versus **1-Cl** (cf., 47.90 ppm, $^1J_{P,Rh} \approx 143.8$ Hz) are consistent with reduction of the metal center and activation of a stronger covalent interaction between P and Rh. Taken together, these data support chemical reduction of **1-Cl** to the formally Rh(I) complex **2** (see Scheme 1).

Dark-red single crystals of **2** suitable for XRD studies were obtained from slow evaporation of a solution of **2** in diethyl ether/toluene. The solid-state structure obtained confirms the reduction of the metal complex implicated by the NMR data. In **2**, the geometry of the formally Rh(I) metal center is distorted square-planar (Figure 3), resulting in a pseudo-C_S molecular geometry. The first coordination sphere around the metal contains both [η^5-Cp*] and [κ^2-PQN]. The angle between the plane defined by the [Cp*] ring and the plane containing Rh, N and P is 84°, indicating that the absence of the single bound chloride anion does not significantly affect this angle. This could be due to the steric bulk of the PQN ligand.

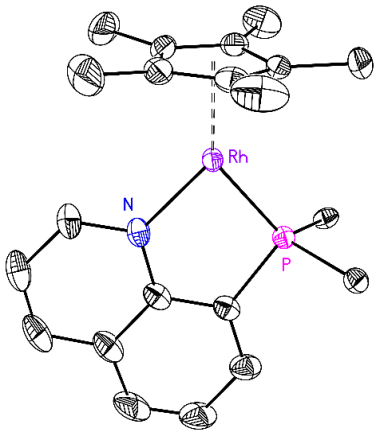

Figure 3. Solid-state structure of **2** (XRD); hydrogen atoms omitted for clarity. Phenyl groups truncated for clarity. Thermal ellipsoids shown at the 50% probability level.

The lowered formal oxidation state of the metal does not significantly alter the C–C bond lengths of the quinoline ligand framework in **2** when compared to the analogous bond lengths in **1** (see SI, Table S2 for bond length comparisons). Thus, the quinoline moiety is likely not serving as a site for significant delocalization of electron density in the reduced complex **2**.[44] However, as there is a continuum between backbonding and formal ligand-centered reduction, both the phosphine and imine moieties are likely to assist in stabilization of the reduced metal center via π-backbonding. Consistent with this picture, the Rh–P, and Rh–N bond lengths contract substantially (by 0.1216 Å and 0.1106 Å, respectively) upon reduction of **1-Cl** to **2**.

To verify that the chemically reduced complex **2** is the product observed in electrochemical reduction of **1-Cl**, cyclic voltammetry data for **2** were collected. In a cathodic scan beginning at E = –1.38 V, the one-electron reduction at ca. –2.3 V is observed; however, the following anodic sweep shows two distinct oxidation waves ($E_{p,a}$ = –1.13, –0.87 V vs. $Fc^{+/0}$), indicating two individual one-electron events. Two corresponding one-electron reductions are observed upon scanning cathodically from the switching potential of ca. –0.25 V. As in the other cases discussed so far, scan rate dependent studies verify that all species present in CVs of **2** are freely diffusing and soluble (Figure S46).

The two quasi-reversible couples measured for **2**, centered at –1.17 V and –0.95 V are assigned to the Rh^{II}/Rh^{I} and Rh^{III}/Rh^{II} reductions, respectively. Notably, these couples are virtually identical to the Rh^{II}/Rh^{I} and Rh^{III}/Rh^{II} reductions measured for **1-NCCH$_3$**; this observation is in accord with our model for the electrochemical behavior of these complexes. Specifically, we conclude that the two, sequential one-electron oxidations of chemically prepared **2** in acetonitrile containing tetrabutylammonium hexafluorophosphate supporting electrolyte lead to formation of $[Cp^*Rh(PQN)NCCH_3]^{2+}$ with hexafluorophosphate counteranions. As this complex is very similar to the chemically prepared analogue **1-NCCH$_3$**, $[Cp^*Rh(PQN)NCCH_3]^{2+}$ with triflate counteranions, these complexes display virtually identical profiles in cyclic voltammetry. This interpretation is corroborated by the peak-to-peak separation (ΔE_p) values measured for the two individual reduction events of **2**. ΔE_p is 140 mV for the more-positive reduction, and 70 mV for the more-negative event; this is consistent with a chemical reaction accompanying the first reduction (loss of the nascent CH_3CN ligand), while the second reduction is virtually reversible (cf. $\Delta E_p(Fc^{+/0})$ = 70 mV under our conditions), suggesting only rapid electron transfer.[45]

The changes in the CV profiles of **1-Cl** and **1-NCCH$_3$**/**2** are unique among the half-sandwich rhodium complexes that we have studied. Compounds in this class bearing bidentate ligands typically show a single, net 2e⁻ reduction from Rh(III) to Rh(I) without formation of a stable Rh(II) intermediate.[6,7b,16,] Reiterating the principles of our working model, the unique behavior of **1-NCCH$_3$** and **2** can be assigned to absence of a chloride ligand. One-electron reduction of **1-Cl** is followed by a chemical reaction that yields a transient Rh(II) complex with a more positive reduction potential than **1-Cl** itself; immediate reduction of this species thus occurs, giving rise to the observed single two-electron wave. In the absence of chloride, however, electrochemical oxidation of **2** generates a different Rh(III) species, bearing a CH_3CN solvent molecule as monodentate ligand. Reduction of this solvento species, $[Cp^*Rh(PQN)(NCCH_3)]^{2+}$, takes place at a more positive potential than for **1-Cl** due to its dicationic nature; evidently, the shift in potential caused by the subsequent chemical reaction (in this case, loss of CH_3CN rather than chloride as in **1-Cl**) is insufficient to cause the transient Rh(II) species to be reduced at a more positive potential than the Rh(III) solvent complex. Thus, two distinct one-electron reductions are measurable, and a metastable rhodium(II) complex is formed near the

electrode. These findings support the overall model for the electrochemical behavior of [Cp*Rh] complexes bearing bidentate ligands, and highlight a significant role for halide ligands in regulation of the electrochemical properties of the metal complexes. In accord with this viewpoint, anionic ligands, like halides, have long been known to decrease the reduction potentials of metal complexes, relative to analogues bearing neutral ligands.[46]

To further confirm the role for halide ligands in regulating the electrochemical properties of these [Cp*Rh] complexes, we titrated a sample of **1-NCCH$_3$** (in the electrochemical cell) with increasing quantities of tetrabutylammonium chloride. The two original reduction waves for **1-NCCH$_3$** are diminished upon chloride addition, while the single, two-electron wave for **1-Cl** centered at –1.19 V grows in intensity (See Figure 4). This confirms rapid conversion of **1-NCCH$_3$** to **1-Cl** by displacement of the ligated solvent with chloride and confirms that the presence/absence of chloride is responsible for the unique appearance of the voltammetric profiles of **1-NCCH$_3$** and **1-Cl**, as the other ligands to the rhodium center, [Cp*] and [PQN], are identical in the two cases.

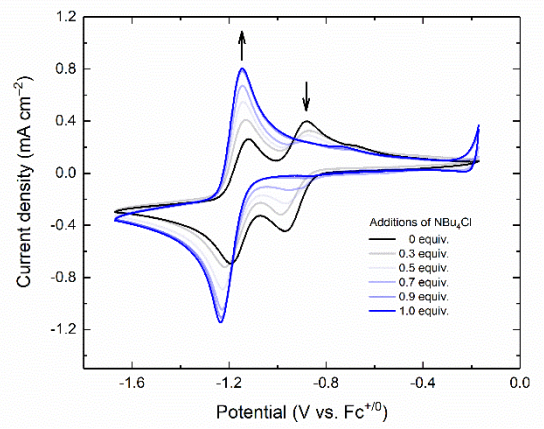

Figure 4. Electrochemical response of **1-NCCH$_3$** in CH_3CN upon addition of various amounts of tetrabutylammonium chloride. Growth of the reduction process with $E_{1/2} = -1.19$ V indicates coordination of chloride to **1-NCCH$_3$** by displacement of bound CH_3CN, giving *in situ* generation of **1-Cl**.

As a complement to this electrochemical titration, we carried out a control electroanalytical study to confirm that chloride was not present as an adventitious impurity in our acetonitrile/tetrabutylammonium hexafluorophosphate electrolyte or isolated samples of **1-NCCH$_3$** and **2**. This was done by potential excursions to check for anodic oxidation of chloride, which is known to occur near +0.75 V vs. $Fc^{+/0}$ in CH_3CN (See SI, Figure S48). We generated a standard curve (Figure S49) with additions of NBu_4Cl, with the result of a linear relationship between [Cl^-] and peak currents measured near 0.75 V. This anodic process is absent in the initial CH_3CN solution containing 0.1 M NBu_4PF_6 supporting electrolyte, confirming a virtually zero baseline for chloride. Furthermore, anodic scans carried out with complexes **1-NCCH$_3$** and **2** do not reveal the presence of any free chloride, as judged by the absence of the key oxidation wave (Figure S50 and S51). Thus, the electrochemical behavior of the [Cp*Rh] complexes can be confidently ascribed to the model discussed above.

Preparation of a [Cp*Rh] Hydride. With **2** in hand, we next examined the possibility of producing a protonated species for comparison to other [Cp*Rh] complexes.[12,21] Upon addition of 1 equiv. of anilinium triflate ($pK_a = 10.6$ in CH_3CN[47]), a solution of **2** drastically lightens to yellow. Following evaporation of volatiles and washing with diethyl ether, a yellow solid is obtained. The ^{1}H NMR spectrum of this material displays an upfield peak at –9.9 ppm that is indicative of a metal hydride complex (Figure S19). The hydride signal appears as a doublet of doublets due to H,Rh and H,P coupling ($J \approx 36.6, 19.9$ Hz). The signal for the [Cp*] protons appears at 1.67 ppm ($^4J_{H,P} \approx 3.1$ Hz; Figure S19). Consistent with the change in oxidation state from Rh(I) to Rh(III), a doublet with a smaller coupling constant ($^1J_{P,Rh} \approx 149.2$ Hz; Figure 5) than in the case of **2** ($^1J_{P,Rh} \approx 246.3$ Hz) is observed in the ^{31}P{^{1}H} NMR spectrum of **3**.

Vapor diffusion of Et_2O into a CH_3CN solution of **3** yielded yellow crystals suitable for XRD studies. The solid state structure of **3** (Figure 5) reveals a return of the Rh(III) center to a pseudo-octahedral geometry. The first coordination sphere around the metal contains the [κ^2-PQN] and [η^5-Cp*] ligands. Gratifyingly, the hydride ligand (H41) could be located in the Fourier difference map, and its position was freely refined. This confirms the direct Rh–H interaction, and identifies **3** as a metal-hydride species.[48] This structure complements another that we recently obtained for an analogous hydride complex supported by the bis(diphenylphosphino)benzene (dppb) ligand.[21]

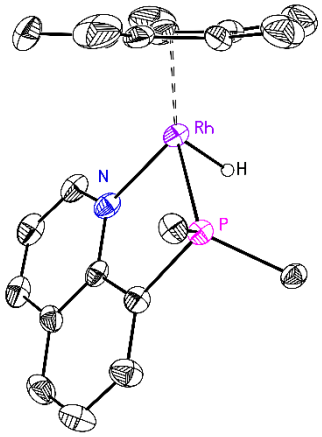

Figure 5. Crystal structure of **3**, triflate counteranion and hydrogen atoms (except for H41) omitted for clarity. Phenyl groups truncated for clarity. Thermal ellipsoids shown at the 50% probability level.

Chemical Reactivity of the [Cp*Rh] Hydride. As previously discussed, [(Cp*H)Rh] complexes generated from Cp*Rh(^{R}bpy) precursors have been isolated and are active for H_2 evolution catalysis.[6,10,11,12,16] The analogous [Cp*Rh–H] generated by protonation of Cp*Rh(dppb) does not react with further equiv. of acid to release H_2.[21] For comparison to these cases, we endeavored to assess the feasibility of release of H_2 from **3** via protonolysis. Treatment of **3** with 1 equiv. of [DMFH]$^+$[OTf]$^-$ ($pK_a \approx 6$ in CH_3CN[49]) leads to slow consumption of the hydride complex **3** and generation of H_2 over 1 h; addition of 3 equiv. leads to complete conversion within 1 h. The metal-containing product of this reactivity is the expected **1-NCCH$_3$**; the disappearance of the upfield ^{1}H NMR signal corresponding to the hydride proton and significant shift of the diagnostic doublet in ^{31}P NMR signal to 50.28 ppm (Figure 6) support this assignment. On the other hand, addition of 10 equiv. of anilinium triflate ($pK_a = 10.6$ in CH_3CN[47]) does not lead to any reactivity as judged by ^{1}H NMR over days, indicating that **3** is resistant to protonolysis by moderately strong acids.

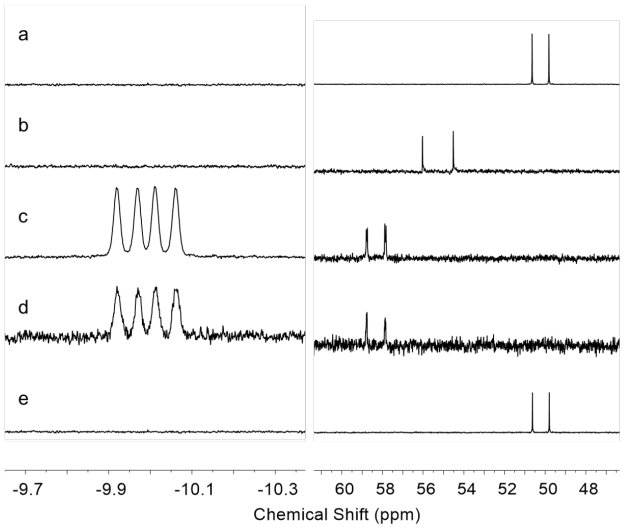

Figure 6. ^{1}H (left) and ^{31}P{^{1}H} (right) NMR spectra : (a) **1-NCCH$_3$**; (b) **2**; (c) **3**; (d) Addition of 10 equiv. anilinium triflate to **3**; (e) Addition of 3 equiv. [DMFH]$^+$[OTf]$^-$ to **3**.

Electrochemical Properties of the [Cp*Rh] Hydride Cyclic voltammetry experiments were carried out to investigate the electron transfer behavior of **3**. The first cathodic sweep of a CV beginning at –0.5 V reveals only an irreversible reduction corresponding to the reduction of the hydride ($E_{p,c}$= –1.75 V vs. Fc$^{+/0}$; see Figure 7). Further scanning to negative potentials reveals an additional reduction at a potential that closely aligns with that of the third reduction of the non-protonated species **2** ($E_{1/2}$ = –2.28 V vs. Fc$^{+/0}$). The returning anodic sweep features two oxidative events corresponding to the two 1e$^-$ couples observed in the voltammogram of **2**. These data are consistent with a fast chemical reaction following 1e$^-$ reduction of **3**, resulting in regeneration of a significant yield of **2**.

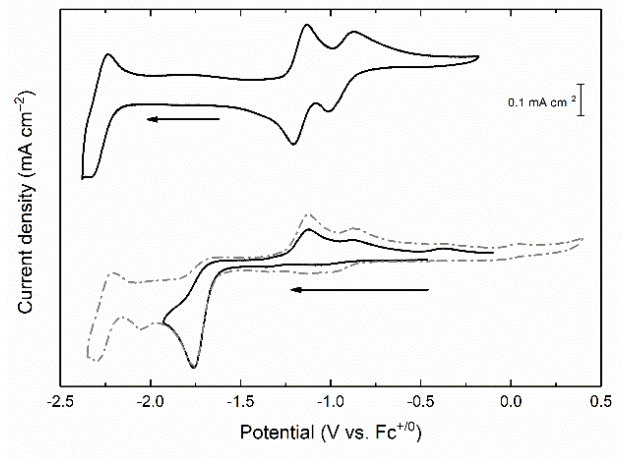

Figure 7. Cyclic voltammetry of **2** (upper panel, 1 mM) and **3** (lower panel, 1 mM). Electrolyte: 0.1 M TBAPF$_6$ in CH$_3$CN, scan rate: 100 mV/s, electrode: highly oriented pyrolytic graphite. The initial potential of the voltammogram of **2** (upper panel) is at ca. –1.38 V, and the initial potential of the voltammogram of **3** (lower panel) is at ca. –0.5 V.

In our recent work with [Cp*Rh] complexes supported by the 1,2-bis(diphenylphosphino)benzene (dppb) ligand, we found that the hydride [Cp*Rh(dppb)H]$^+$ undergoes metal centered reduction at –2.34 V vs. Fc$^{+/0}$.[21] This quite negative potential contrasts with the more positive potentials (–1.45 and –1.73 V) encountered for reductions of [Cp*H] complexes supported by 2,2′-bipyridyl.[12] These reductions are centered on the bpy ligands, as a result of presence of low-lying, delocalized π* orbitals.[50] Similarly, in the case of hydride **3** supported by the PQN ligand, a significantly more positive reduction potential ($E_{p,c}$ = –1.75 V) is observed in comparison to that of the metal-centered reduction of [Cp*Rh(dppb)H]$^+$. Thus, there is likely significant ligand involvement in the reduction measured for the hydride **3** at $E_{p,c}$ = –1.75 V.

For comparison, cyclic voltammetry collected with the metal-free PQN ligand revealed a quasireversible reduction at –2.46 V vs. Fc$^{+/0}$ (See SI, Figure S54). A second oxidation wave was also observed at a more positive potential (–1.17 V vs. Fc$^{+/0}$) following reduction. These findings regarding reduction potentials are consistent with a shift of the ligand reduction to a significantly more positive value upon binding to the Lewis acidic Rh(III) center (cf. ligand-centered reduction of [(Cp*H)Rh(^{H}bpy)]$^+$ at = –1.74 V vs. –2.57 V for free ^{H}bpy).[12,40] Confirming this assignment of ligand-centered reduction of **3**, prior work with PQN complexes of ruthenium has implicated ligand-centered reductions at similar potentials, through comparisons with diphosphine and diimine ligated complexes.[28a]

Electrochemical Generation of the [Cp*Rh] Hydride in the Presence of Acid. The observation that **2**, the product of two-electron reduction of **1-Cl**, can be readily protonated to prepare and isolate hydride **3** suggested to use that we might probe this hydride-forming reactivity under electrochemical conditions. Thus, we targeted an experiment in which **1-Cl** would be reduced electrochemically in the presence of a proton source, a situation that should lead to production of **3** *in situ*. However, a suitable organic acid must be carefully selected in such efforts. Anilinium triflate was used for synthesis of **3** in the preparative work, but this acid undergoes direct reduction at relatively positive potentials on carbon electrodes ($E_{p,c}$= –1.58 vs. Fc$^{+/0}$).[16] Such reactivity would interfere with observation of the reduction of **3** produced *in situ* ($E_{p,c}$= –1.75 V vs. Fc$^{+/0}$). Thus, triethylammonium triflate (pK_a = 18.8 in CH$_3$CN[47]) was chosen for this electrochemical study instead. Notably, we confirmed that treatment of **2** with excess triethylammonium does indeed lead to generation of **3** (as judged by ^{1}H NMR spectra), and thus this weaker acid is amenable to electrochemical studies.

Aliquots of a 1:1 mixture of [Et$_3$NH]$^+$/Et$_3$N solution were added to **1-Cl** and cyclic voltammograms collected for each addition (Figure 8). As the acid solution was added, an increasingly irreversible response was recorded for the Rh(III)/Rh(I) couple previously measured for **1-Cl** (cf., Figure 2). The shape of the cathodic two-electron wave becomes distorted upon acid addition, likely due to activation of one or more coupled chemical reactions taking place between the reduced complex(es) and the added acid. Concurrently, a new irreversible reduction wave appears at –1.75 V. This reduction wave occurs at a virtually identical potential to that of the reduction wave measured for the chemically-prepared hydride **3** (cf., voltammetry data in Figure 7). Thus, we conclude that hydride **3** can be generated *in situ* by reduction of **1-Cl** and subsequent reaction with triethylammonium.

Upon further additions of the buffered acid, the current flow associated with reduction of **2** is modestly enhanced, slightly beyond the current associated with reduction of **3** alone. Enhancement is observed upon addition of up to 7 equiv. of [Et$_3$NH]$^+$/Et$_3$N ($j_{cat}/(j_p/2) \approx 1.5$; Figure 8, inset).[51] We note that insignificant current is associated with background reduction of triethylammonium at these potentials (see SI, Figure S56). The modest enhancement of the reductive current at –1.75 V suggested to us that conversion of H$^+$ to H$_2$ mediated by a reduced form of **3** might be occurring.

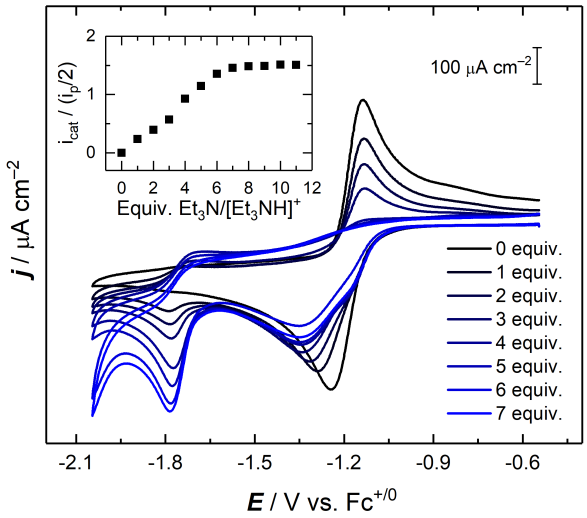

Figure 8. Cyclic voltammetry of 1 with 1 equv. of $[Et_3NH]^+$/Et3N in 50μL additions (CH_3CN, 0.1 M $[nBu_4N][PF_6]$, 100 mV/s). (Inset): Plot of icat/(ip/2) vs equivalents (mMol) of $[Et_3NH]^+$/Et_3N added.

Thus, we next moved to carry out bulk electrolysis experiments to assess the possibility of H_2 production. Controlled potential electrolysis (CPE) of **1-Cl** (see SI, Figure S60 for chronoamperogram) in the presence of 10 equiv. of $[Et_3NH]^+$ was carried out for 1.5 h. at –1.75 V vs. $Fc^{+/0}$, resulting in the passage of 29.1 C of charge. Sampling of the headspace of the electrolysis cell by gas chromatography revealed generation of H_2 with a low 34% Faradaic efficiency. The total amount of H_2 evolved equates to a very low turnover number (TON; mol H_2 detected per mol [Rh]) of only 1.3, while the low Faradaic yield indicates involvement of unproductive side reactions under these conditions. A similar CPE experiment (Figure S59) carried out with **1-NCCH$_3$** under identical conditions reveals a similarly low Faradaic efficiency of 36%, confirming the poor H_2 evolving properties of these complexes, regardless of the presence of chloride or bound solvent ligands in the precatalysts. ^{1}H NMR spectra collected on the working solution following electrolysis of **1-NCCH$_3$** or **1-Cl** with added acid show that the dominant Rh-containing component of the solution is the hydride **3**; however, there are also small new peaks in the aromatic region of the spectra (see SI, Figures S33 and S34), suggesting formation of secondary side products during electrolysis. Likewise, electrolysis of isolated **3** for 1.5 h at –1.75 V vs. $Fc^{+/0}$ reveals no production of H_2 as judged by gas chromatography. However, a product of this electrolysis of **3** is **2**, as judged by UV-visible spectroscopy (see SI for data, Figure S38), suggesting reactivity upon reduction that does not lead to H_2 production. Taken together, these results show that the reductive electrochemical reactivity of the hydride is not clean (whether chemically prepared or formed *in situ*) and does not lead to reliable H_2 generation.

To further probe this reactivity, we attempted chemical reduction of hydride **3** with decamethylcobaltocene (Cp^*_2Co, E = –1.94 V vs. $Fc^{+/0}$,[43] 1 equiv.). In line with conclusions drawn from the bulk electrolysis experiments, we observed null generation of H_2 by headspace analysis, and the presence of multiple P-containing by-products by $^{31}P\{^1H\}$ NMR (see SI, Figure S32). No solids or heterogeneous material were visible. We also carried out a companion chemical reduction of **3** in the presence of both 1 equiv. of Cp^*_2Co and 1 equiv. of $[Et_3NH]^+$. This experiment revealed formation of null H_2 by GC, along with **3** and other byproducts by ^{1}H and $^{31}P\{^1H\}$ NMR (see SI, Figures S35 and S36, respectively). Thus, we conclude that both in the presence and absence of exogeneous acid, and under both chemical and electrochemical conditions, hydride **3** is not effective for H_2 generation.

CONCLUSIONS

Introduction of the mixed [*P,N*]-donor ligand PQN engenders substantial changes in the properties of [Cp*Rh] complexes supported by this framework in comparison to those previously reported for [*P,P*]- and [*N,N*]-ligated systems. Modulation of the electrochemical properties of the [Cp*Rh] fragment is perhaps the most striking change, as preparation of the solvento complex **1-NCCH$_3$** and related reduced complex **2** enable observation of two, sequential, quasi-reversible one-electron reductions. This behavior contrasts with the single two-electron reduction events measured most commonly for [Cp*Rh] complexes bearing diphosphine and diimine ligands. Treatment of Cp*Rh(PQN) (**2**) with acid results in generation of hydride complex **3**, which is resistant to protonolysis by the moderate acid anilinium triflate. Electrochemical studies show that **3** undergoes ligand-centered reduction at –1.75 V, inducing further reactivity. However, chemical and electrochemical reduction experiments show that this reactivity does not lead to effective H_2 generation. This contrasts with the robust and effective catalysis afforded by [Cp*Rh] complexes bearing diimine ligands and suggests that the [Cp*] ligand-centered protonation events associated with these diimine complexes may be crucial for effective H_2 generation in this broadly useful family of complexes.

EXPERIMENTAL SECTION

General Considerations. All manipulations were carried out in dry N_2-filled gloveboxes (Vacuum Atmospheres Co., Hawthorne, CA) or under N_2 atmosphere using standard Schlenk techniques unless otherwise noted. All solvents were of commercial grade and dried over activated alumina using a PPT Glass Contour (Nashua, NH) solvent purification system prior to use, and were stored over molecular sieves. All chemicals were from major commercial suppliers and used as received after extensive drying. $[Cp^*RhCl_2]_2$ was prepared according to literature procedure.[32] The PQN ligand was synthesized by the method of Haftendorn[34] and purified by the method of Metzger.[35] Deuterated NMR solvents were purchased from Cambridge Isotope Laboratories; CD_3CN was dried over molecular sieves and C_6D_6 was dried over sodium/benzophenone. ^{1}H, ^{13}C, ^{19}F, and ^{31}P NMR spectra were collected on 400 or 500 MHz Bruker spectrometers and referenced to the residual protio-solvent signal[52] in the case of ^{1}H and ^{13}C. Heteronuclear NMR spectra were referenced to the appropriate external standard following the recommended scale based on ratios of absolute frequencies (Ξ).[53,54] ^{19}F NMR spectra are reported relative to CCl_3F, and ^{31}P NMR spectra are reported relative to H_3PO_4. Chemical shifts (δ) are reported in units of ppm and coupling constants (J) are reported in Hz. Electronic absorption spectra were collected with an Ocean Optics Flame spectrometer, in a 1-cm pathlength quartz cuvette. Elemental analyses were performed by Midwest Microlab, Inc. (Indianapolis, IN).

Electrochemistry. Electrochemical experiments were carried out in a nitrogen-filled glove box. 0.10 M tetra(n-butylammonium)hexafluorophosphate (Sigma-Aldrich; electrochemical grade) in acetonitrile served as the supporting electrolyte. Measurements were made with a Gamry Reference 600 Plus Potentiostat/Galvanostat using a standard three-electrode configuration. The working electrode was the basal plane of highly oriented pyrolytic graphite (HOPG) (GraphiteStore.com, Buffalo Grove, Ill.; surface area: 0.09 cm^2), the counter electrode was a platinum wire (Kurt J. Lesker, Jefferson Hills, PA; 99.99%, 0.5 mm diameter), and a silver wire immersed in electrolyte served as a pseudo-reference electrode (CH Instruments). The reference was separated from the working solution by a Vycor frit (Bioanalytical Systems, Inc.). Ferrocene (Sigma Aldrich; twice-sublimed) was added to the electrolyte solution at the conclusion of each experiment (~1 mM); the midpoint potential of the ferrocenium/ferrocene couple (denoted as $Fc^{+/0}$) served as an external standard for comparison of the recorded potentials. Concentrations of analyte for cyclic voltammetry were typically 1 mM. In most cases (except those involving acid additions), the second full sweep of voltammetry is shown.

Synthetic Procedures.

Synthesis of 1-Cl. To a suspension of $[Cp^*RhCl_2]_2$ in CH_3CN (0.4815 g, 0.0779. mmol) were added AgOTf (0.0552 g, 0.219 mmol, 2 equiv) in CH_3CN and PQN (0.5000 g, 0.319 mmol, 2.05 equiv) as a THF solution. The color of the reaction mixture rapidly changed from brick-red to orange, and a yellow precipitate formed. After 15 min, the suspension was filtered to remove the AgOTf byproduct, and the volume of the filtrate was reduced to ~1 mL. Addition of Et_2O (~80 mL) caused precipitation of a yellow solid, which was collected by filtration. Pure material was obtained via crystallization by vapor diffusion of Et_2O into a concentrated CH_3CN solution of the title compound (0.6807 g, 57.9%). The same strategy was employed to obtain single-crystals suitable for X-ray diffraction studies. ^{1}H NMR (500 MHz, CD_3CN) δ 9.10 (d, *J* = 5.2 Hz, 1H, *H1*), 8.68 (d, *J* = 8.4 Hz, 1H, *H3*), 8.30 (d, *J* = 8.2 Hz, 1H, *H5*), 8.27 – 8.22 (m, 1H, *H7*), 7.97 – 7.90 (m, 2H, *H11, H6*), 7.89 – 7.81 (m, 2H, *H2*), 7.67 (td, *J* = 7.2, 1.8 Hz, 1H, *H13*), 7.63 – 7.53 (m, 3H, *H12, H17*), 7.45 (td, *J* = 7.9, 2.6 Hz, 2H, *H16*), 7.18 – 7.11 (m, 2H, *H15*), 1.54 (d, *J* = 3.7 Hz, 15H, *H19*) ppm. ^{13}C{^{1}H} NMR (126 MHz, CD_3CN) δ 158.15 (s, *C1*), 151.64 (d, *J* = 21.37 Hz, *C9*), 140.31 (d, *J* = 2.2 Hz, *C3*), 138.81 (d, *J* = 2.7 Hz, *C7*), 135.05 (d, *J* = 11.2 Hz, *C11*), 133.27 (d, *J* = 2.6 Hz, *C5*), 132.78 (d, *J* = 10.8 Hz, *C15*), 132.15 (d, *J* = 3.3 Hz, *C13*), 131.94 (d, *J* = 48.7 Hz, *C14 or C8*), 131.15(d, *J* = 50.3 Hz, *C8 or C14*), 131.70 (d, *J* = 3.4 Hz, *C17*), 129.77 (d, *J* = 9.0 Hz *C4*), 128.89 (s, *C16*), 128.88 (d, *J* = 4.0 Hz *C6*), 128.80 (d, *J* = 11.4 Hz, *C12*), 124.83 (d, *J* = 55.4 Hz *C10*), 124.57 (s, *C2*), 101.77 (dd, *J* = 6.8 Hz, *J* = 3.0 Hz *C18*), 8.38 (m, *C19*) ppm. ^{19}F NMR (376 MHz, CD_3CN) δ –79.36 ppm. ^{31}P{^{1}H} NMR (162 MHz, CD_3CN) δ 47.90 (d, *J* = 143.8 Hz).ppm. Electronic absorption spectrum (CH_3CN): 366 nm (4323 M^{-1} cm^{-1}). ESI-MS (positive) *m/z*: 550.09 [**1-Cl** – Cl^- – OTf^-]$^+$, 586.07 [**1-Cl** – OTf^-]$^+$. Anal. Calcd. for $C_{40}H_{39}ClF_6P_3Rh$: C, 52.22; H, 4.25, N, 1.90. Found: C, 52.02; H, 4.31, N, 1.89.

Synthesis of 1-NCCH$_3$. A solution of **1** in CH_3CN (0. 0324 g, 0.0041 mmol) and a solution of AgOTf in CH_3CN (0. 0103 g, 0.0081 mmol) were combined and stirred for 1.5 hours, during which time the solution turned light yellow and a white precipitate formed. The of AgCl byproduct was removed by filtration over celite, and subsequent removal of volatiles *in vacuo* provides the title compound as a yellow solid (0.0324g, >99% yeild). ^{1}H NMR (500 MHz, CD_3CN) δ9.25 (d, *J* = 5.2 Hz, 1H), 8.90 (dt, *J* = 8.4, 1.7 Hz, 1H), 8.53 (dt, *J* = 8.2, 1.5 Hz, 1H), 8.31 (ddd, *J* = 10.2, 7.2, 1.3 Hz, 1H), 8.07 (ddd, *J* = 8.1, 7.2, 1.6 Hz, 2H), 8.02 (dd, *J* = 8.3, 5.2 Hz, 1H) 7.80 – 7.52 (m, 7H), 7.49 – 7.37 (m, 2H), 1.62 (d, *J* = 3.8 Hz, 15H) ppm. ^{13}C{^{1}H} NMR (126 MHz, CD_3CN) δ 159.21 (s), 152.97 (d, *J* = 20.7 Hz), 142.35 (s) 141.53 (s), 135.08 (d, *J* = 2.5 Hz), 134.19 (d, *J* = 10.9 Hz), 133.86 (d, *J* = 10.9 H), 133.64 (d, *J* = 3.5 Hz), 133.08 (d, *J* = 3.1 Hz), 131.34 (d, *J* = 9.1 Hz),130.20 (dd, *J* = 14.9, 11.4 Hz), 130.04 (s), 129.72 (s), 129.31 (s), 126.89 (d, *J* = 53.0 Hz), 126.07 (s), 125.93 (d, *J* = 52.6 Hz), 123.04 (s), 120.49 (s), 104.95 – 104.84 (m), 9.20 (s), ppm. ^{19}F NMR (376 MHz, CD_3CN) δ -79.30. ^{31}P{^{1}H} NMR (162 MHz, C_6D_6) δ 50.26 (d, *J* = 134.0 Hz) ppm. ESI-MS (positive) *m/z*: 550.09 [**1-NCCH$_3$** – CH_3CN – OTf^-]$^+$.

Synthesis of 2. A solution of **1** in a 1:1 mixture of THF/CH_3CN and a solution of Cp_2Co in THF (0.0491 g, 0.0178 mmol) was added to a 'thawing' solution of **1** (0. 1000 g, 0.0043 mmol) and stirred for 3 hours, during which time the yellow solution became a dark red. The volatiles removed *in vacuo*. Extraction with hexane and removal of the volatiles *in vacuo* provides the title compound as a dark red solid (00410g, 54.7%). Single-crystals suitable for X-ray diffraction studies were obtained by slow evaporation of Et_2O and toluene at -35°C. ^{1}H NMR (400 MHz, C_6D_6) δ 8.69 (d, *J* = 5.5 Hz, 1H, *H1*), 7.81 (dd, *J* = 10.5, 7.6 Hz , 4H, *H11*), 7.54 (t, *J* = 7.5 Hz, 1H, *H5*), 7.21 (d, *J* = 8.3 Hz, 1H, *H3*), 7.13 – 7.05 (m, 4H overlaps with solvent residual, *H12*), 7.09 (m, 2H, *H13*), 7.00 (d, *J* = 7.5 Hz, 1H, *H7*), 6.77 (t, *J* = 7.4 Hz, 1H, *H6*), 6.18 (dd, *J* = 8.1, 5.5 Hz, 1H, *H2*). 1.98 (d, *J* = 1.9 Hz, 15H) ppm. ^{13}C NMR (126 MHz, C_6D_6) δ 155.33 (d, *J* = 24.3 Hz, *C9*), 150.67 (s, *C1*), 139.74 (d, *J* = 35.74 Hz, *C10*), 139.30 (d, *J* = 26.3 Hz, *C8*), 133.07 (d, *J* = 13.6 Hz, *C11*), 132.90 (s, *C5*), 128.89 (s, *C4*), 128.75 (s, *C7*), 128.66 (s, *C13*), 127.26 (d, *J* = 4.5 Hz, *C6),* 124.40 (s, *C2*), 123.40 (s, *C3*), (obscured by solvent peak, *C12*), 92.65 (s, *C14*), 10.93(s, *C15*), ppm. ^{31}P{^{1}H} NMR (162 MHz, C_6D_6) δ 55.29 (d, *J* = 245.0 Hz) ppm. Electronic absorption spectrum (CH_3CN): 478 nm (2,500 M^{-1} cm^{-1}).

Synthesis of 3. A solution of anilinium triflate CH_3CN (0.0185 g, 0.0035 mmol, 1 equiv) was added to a suspension of **2** in (0.0086g, 0.0071 mmol). The solution became light yellow immediately. Volatiles were removed *in vacuo*. Washing with hexanes followed by filtration removal of volatiles yielded the title compound as a light-yellow solid (0.0170g, 72.0%). Single-crystals suitable for X-ray diffraction studies were obtained by vapor diffusion of Et_2O into a CH_3CN solution of the title compound. ^{1}H NMR (400 MHz, CD_3CN) δ 8.90 (d, *J* = 5.1 Hz, 1H, *H1*), 8.55 (d, *J* = 8.4 Hz, 1H, *H3*), 8.29 (dd, *J* = 9.5, 7.5 Hz, 1H, *H7*), 8.23 – 8.13 (m, 3H, *H5, H12*), 7.86 – 7.78 (m, 1H, *H6*), 7.75 – 7.65 (m, 4H, *H2, H11, H13*), 7.55 (dt, *J* = 7.4, 4.1 Hz, 1H, *H17*), 7.48 (dt, *J* = 7.5, 3.8 Hz, 2H, *H16*), 7.22 – 7.04 (m, 2H, H15), 1.70 (dd, *J* = 3.1, 1.4 Hz, 15H, *H19*), –9.9 (dd, *J* = 36.6, 19.9 Hz, 1H,), ppm. ^{13}C{^{1}H} NMR (126 MHz, CD_3CN) δ 157.53 (s, *C1*), 151.86 (s, *C9*), 138.98 (s, *C3*), 137.13 (s, *C7*), 135.79 (dd, *J* = 13.1, 2.0 Hz, *C10*) 134.3 (d, *J* = 49.05 Hz, *C8*), 132.79 (d, *J* = 48.76 Hz, *C14*), 132.42 (d, *J* = 2.9 Hz, *C5*), 132.38 (s, *C13*), 131.90 (d, *J* = 11.3 Hz, *C15*), 130.82 (s, *C17*), 129.74 (s, *C4*), 129.13 (d, *J* = 11.7 Hz, *C11*), 128.92 (s, *C6*), 128.80(s, *C12*), 128.76 (d, *J* = 1.8 Hz, *C16*), 123.99 (s, *C2*), 100.07 (dd, *J* = 5.4, 3.1 Hz), *C18*), 8.79 (s, *C19*) ppm. ^{19}F NMR (376 MHz, CD_3CN) δ –79.37 ppm. ^{31}P{^{1}H} NMR (162 MHz, CD_3CN) δ 57.49 (dd, *J* = 148.0, 8.2 Hz) ppm. Electronic absorption spectrum (CH_3CN): 404 nm (1,912 M^{-1} cm^{-1}). Anal. Calcd. for $C_{41}H_{40}O_3F_3P_2SRh$: C, 54.79; H, 4.60, N, 2.00. Found: C, 54.64; H, 4.52, N, 2.04.

ASSOCIATED CONTENT

Supporting Information

The Supporting Information is available free of charge on the ACS Publications website.

NMR spectra and characterization of complexes; additional electrochemical, UV-visible, reactivity, and X-ray crystallographic data (PDF)

Cartesian coordinates (XYZ)

Accession Codes

CCDC 1858633–1858635 contain the supplementary crystallographic data for this paper.

AUTHOR INFORMATION

Corresponding Author

* To whom correspondence should be addressed. E-mail: blakemore@ku.edu; phone: +1-785-864-3019.

Notes

The authors declare no competing financial interests.

ACKNOWLEDGMENT

The authors thank Dr. Justin Douglas and Sarah Neuenswander for assistance with NMR spectroscopy. This work was supported by the US National Science Foundation through award OIA-1833087, and by the University of Kansas. Preliminary work on this project was supported by the US National Science Foundation through the NSF REU Program in Chemistry at the University of Kansas (CHE-1560279). Support for NMR instrumentation was provided by NIH Shared Instrumentation Grants S10OD016360 and S10RR024664, and by an NSF MRI grant CHE-1625923.

REFERENCES

[1] (a) Rosenthal, J.; Nocera, D. G., Role of Proton-Coupled Electron Transfer in O–O Bond Activation. *Acc. Chem. Res.* **2007,** *40*, 543-553. (b) Huynh, M. H. V.; Meyer, T. J., Proton-Coupled Electron Transfer. *Chem. Rev.* **2007,** *107*, 5004-5064. (c) Roth, J. P.; Yoder, J. C.; Won, T.-J.; Mayer, J. M., Application of the Marcus Cross Relation to Hydrogen Atom Transfer Reactions. *Science* **2001,** *294*, 2524-2526

[2] (a) Kaesz, H. D.; Saillant, R. B., Hydride complexes of the transition metals. *Chem. Rev.* **1972,** *72*, 231-281. (b) Jordan, A. J.; Lalic, G.; Sadighi, J. P., Coinage Metal Hydrides: Synthesis, Characterization, and Reactivity. *Chem. Rev.* **2016,** *116*, 8318-8372.

[3] Khusnutdinova, J. R.; Milstein, D., Metal-Ligand Cooperation. *Angew. Chem. Int. Ed.* **2015,** *54*, 12236-12273.

[4] (a) Warren, J. J.; Tronic, T. A.; Mayer, J. M., Thermochemistry of Proton-Coupled Electron Transfer Reagents and its Implications. *Chem. Rev.* **2010,** *110*, 6961-7001. (b) Huynh, M. H. V.; Meyer, T. J., Proton-Coupled Electron Transfer. *Chem. Rev.* **2007**, 107, 5004-5064. (c) Krishtalik, L. I., Energetics of multielectron reactions. Photosynthetic oxygen evolution. *Biochim. Biophys. Acta, Bioenerg.* **1986**, *849*, 162-171. (d) Chirik, P. J.; Wieghardt, K., Radical Ligands Confer Nobility on Base-Metal Catalysts. *Science* **2010,** *327*, 794-795.

[5] (a) Lyaskovskyy, V.; de Bruin, B., Redox Non-Innocent Ligands: Versatile New Tools to Control Catalytic Reactions. *ACS Catal.* **2012,** *2*, 270-279. (b) Luca, O. R.; Crabtree, R. H., Redox-active ligands in catalysis. *Chem. Soc. Rev.* **2013,** *42*, 1440-1459. (c) Chirik, P. J., Preface: Forum on Redox-Active Ligands. *Inorg. Chem.* **2011,** *50*, 9737-974.

[6] (a) U. Kölle and M. Grätzel, *Angew. Chem.*, 1987, **99**, 572-574. (b) U. Kölle and M. Grätzel, *Angew. Chem. Int. Ed. Engl.*, 1987, **26**, 567-570.

[7] Kölle, U.; Kang, B. S.; Infelta, P.; Comte, P.; Grätzel, M., Electrochemical and Pulse-Radiolytic Reduction of (Pentamethylcyclopentadienyl)(Polypyridyl)Rhodium Complexes. *Chem. Ber.* **1989,** *122*, 1869-1880.

[8] (a) Ruppert, R.; Herrmann, S.; Steckhan, E., Efficient Indirect Electrochemical Insitu Regeneration of Nadh - Electrochemically Driven Enzymatic Reduction of Pyruvate Catalyzed by D-Ldh. *Tetrahedron Lett.* **1987,** *28*, 6583-6586. (b) Lo, H. C.; Leiva, C.; Buriez, O.; Kerr, J. B.; Olmstead, M. M.; Fish, R. H., Bioorganometallic chemistry. 13. Regioselective reduction of NAD(+) models, 1-benzylnicotinamde triflate and beta-nicotinamide ribose-5 '-methyl phosphate, with in situ generated [CP*Rh(Bpy)H](+): Structure-activity relationships, kinetics, and mechanistic aspects in the formation of the 1,4-NADH derivatives. *Inorg. Chem.* **2001,** *40*, 6705-6716.

[9] (a) Steckhan, E.; Herrmann, S.; Ruppert, R.; Dietz, E.; Frede, M.; Spika, E., Analytical Study of a Series of Substituted (2,2'-Bipyridyl)(Pentamethylcyclopentadienyl)Rhodium and Iridium Complexes with Regard to Their Effectiveness as Redox Catalysts for the Indirect Electrochemical and Chemical-Reduction of Nad(P)+. *Organometallics* **1991,** *10*, 1568-1577. (b) Fukuzumi, S.; Kobayashi, T.; Suenobu, T., Efficient Catalytic Decomposition of Formic Acid for the Selective Generation of H-2 and H/D Exchange with a Water-Soluble Rhodium Complex in Aqueous Solution. *ChemSusChem* **2008,** *1*, 827-834.

[10] Quintana, L. M. A.; Johnson, S. I.; Corona, S. L.; Villatoro, W.; Goddard, W. A.; Takase, M. K.; VanderVelde, D. G.; Winkler, J. R.; Gray, H. B.; Blakemore, J. D., Proton-hydride tautomerism in hydrogen evolution catalysis. *Proc. Natl. Acad. Sci. USA* **2016,** *113*, 6409-6414.

[11] Pitman, C. L.; Finster, O. N. L.; Miller, A. J. M., Cyclopentadiene-mediated hydride transfer from rhodium complexes. *Chem. Commun.* **2016,** *52*, 9105-9108.

[12] Peng, Y.; Ramos-Garces, M. V.; Lionetti, D.; Blakemore, J. D., Structural and Electrochemical Consequences of [Cp*] Ligand Protonation. *Inorg. Chem.* **2017,** *56*, 10824-10831.

[13] (a) Kefalidis, C. E.; Perrin, L.; Burns, C. J.; Berg, D. J.; Maron, L.; Andersen, R. A., Can a pentamethylcyclopentadienyl ligand act as a proton-relay in f-element chemistry? Insights from a joint experimental/theoretical study. *Dalton Trans.* **2015,** *44*, 2575-2587. (b) O, W. W. N.; Lough, A. J.; Morris, R. H., Bifunctional Mechanism with Unconventional Intermediates for the Hydrogenation of Ketones Catalyzed by an Iridium(III) Complex Containing an N-Heterocyclic Carbene with a Primary Amine Donor. *Organometallics* **2012,** *31*, 2152-2165.

[14] (a) Chalkley, M. J.; Del Castillo, T. J.; Matson, B. D.; Roddy, J. P.; Peters, J. C., Catalytic N2-to-NH3 Conversion by Fe at Lower Driving Force: A Proposed Role for Metallocene-Mediated PCET. *ACS Central Science* **2017,** *3*, 217-223. (b) Chalkley, M. J.; Del Castillo, T. J.; Matson, B. D.; Peters, J. C., Fe-Mediated Nitrogen Fixation with a Metallocene Mediator: Exploring pKa Effects and Demonstrating Electrocatalysis. *J. Am. Chem. Soc.* **2018,** *140*, 6122-6129.

[15] Pal, S.; Kusumoto, S.; Nozaki, K., Dehydrogenation of Dimethylamine–Borane Catalyzed by Half-Sandwich Ir and Rh Complexes: Mechanism and the Role of Cp* Noninnocence. *Organometallics* **2018,** *37*, 906-914.

[16] Henke, W. C.; Lionetti, D.; Moore, W. N. G.; Hopkins, J. A.; Day, V. W.; Blakemore, J. D., Ligand Substituents Govern the Efficiency and Mechanistic Path of Hydrogen Production with [Cp*Rh] Catalysts. *ChemSusChem* **2017,** *10*, 4589-4598.

[17] Creutz, C., Bipyridine radical ions. *Comments Inorg. Chem.* **1982,** *1*, 293-311.

[18] (a) Halpern, J.; Peters, E., Mechanism of the Catalytic Activation of Molecular Hydrogen by Metal Ions. *J. Chem. Phys.* **1955,** *23*, 605-605. (b) Dempsey, J. L.; Winkler, J. R.; Gray, H. B., Mechanism of H2 Evolution from a Photogenerated Hydridocobaloxime. *J. Am. Chem. Soc.* **2010,** *132*, 16774-16776.

[19] (a) Klingert, B.; Werner, H., Basische Metalle, XLII. Die Metall-Basizität der Komplexe C5Me5Rh(PMe3)2, C5Me5Rh(C2H4PMe3 und C5Me5Rh(C2H4)P2Me4: Neue Pentamethyl-cyclopentadienylrhodium(I)- und -rhodium(III)-Verbindungen. *Chem. Ber.* **1983,** *116*, 1450-1462. (b) Faller, J. W.; D'Alliessi, D. G., Tunable Stereoselective Hydrosilylation of PhC∶CH Catalyzed by Cp*Rh Complexes. *Organometallics* **2002,** *21*, 1743-1746.

[20] Faraone, F.; Bruno, G.; Schiavo, S. L.; Tresoldi, G.; Bombieri, G., η5-Cyclopentadienylrhodium(I) complexes containing diphosphines and their reactions with the electrophiles H+ and Me+. Crystal and molecular structure of [Rh(η-C5H5)(CO)(Ph2PCH2PPh2)], a

complex with a unidentate bis(diphenylphosphino)methane ligand. *J. Chem. Soc., Dalton Trans.* **1983,** 433-438.

[21] Boyd, E. A.; Lionetti, D.; Henke, W. C.; Day, V. W.; Blakemore, J. D., Preparation, Characterization, and Electrochemical Activation of a Model [Cp*Rh] Hydride. *Inorg. Chem.* **2018**, DOI: 10.1021/acs.inorgchem.8b02160

[22] (a) Canovese, L.; Visentin, F.; Santo, C.; Chessa, G.; Bertolasi, V., Allyl Amination of Phosphinoquinoline Allyl Complexes of Palladium. Influence of the Allyl Hapticity on the Reaction Rate and Regiochemistry. *Organometallics* **2010,** *29*, 3027-3038. (b) Suzuki, T., Crystal and Molecular Structures of Bis[8-(diphenylphosphino)quinoline]palladium(II) Complexes: $Pd(Ph_2Pqn)_2XY$ (XY = Cl_2, Br_2 or $ClBF_4$). *Bull. Chem. Soc. Jpn.* **2004,** *77*, 1869-1876

[23] Wehman, P.; van Donge, H. M. A.; Hagos, A.; Kamer, P. C. J.; van Leeuwen, P. W. N. M., *J. Organomet. Chem.* **1997,** *535*, 183-193.

[24] Suzuki, T.; Yamaguchi, H.; Fujiki, M.; Hashimoto, A.; Takagi, H. D., Crystal structures of dichloridopalladium(II), -platinum(II) and -rhodium(III) complexes containing 8-(diphenylphosphanyl)quinoline. *Acta Cryst. Sec. E* **2015,** *71*, 447-451.

[25] (a) Suzuki, T.; Yamaguchi, H.; Hashimoto, A.; Nozaki, K.; Doi, M.; Inazumi, N.; Ikeda, N.; Kawata, S.; Kojima, M.; Takagi, H. D., Orange and Yellow Crystals of Copper(I) Complexes Bearing 8-(Diphenylphosphino)quinoline: A Pair of Distortion Isomers of an Intrinsic Tetrahedral Complex. *Inorg. Chem.* **2011,** *50*, 3981-3987. (b) Mondal, R.; Lozada, I. B.; Davis, R. L.; Williams, J. A. G.; Herbert, D. E., Site-Selective Benzannulation of N-Heterocycles in Bidentate Ligands Leads to Blue-Shifted Emission from [(P^N)Cu]2(μ-X)2 Dimers. *Inorg. Chem.* **2018,** *57*, 4966-4978.

[26] Akira, H.; Hiroshi, Y.; Takayoshi, S.; Kazuo, K.; Masaaki, K.; D., T. H., Preparation, Crystal Structures, and Spectroscopic and Redox Properties of Nickel(II) Complexes Containing Phosphane–(Amine or Quinoline)-Type Hybrid Ligands and a Nickel(I) Complex Bearing 8-(Diphenylphosphanyl)quinoline. *Eur. J. Inorg. Chem.* **2010,** *2010*, 39-47.

[27] Huang, L.; Rominger, F.; Rudolph, M.; Hashmi, A. S. K., A general access to organogold(iii) complexes by oxidative addition of diazonium salts. *Chem. Commun.* **2016,** *52*, 6435-6438.

[28] (a) Nakamura, G.; Okamura, M.; Yoshida, M.; Suzuki, T.; Takagi, H. D.; Kondo, M.; Masaoka, S., Electrochemical Behavior of Phosphine-Substituted Ruthenium(II) Polypyridine Complexes with a Single Labile Ligand. *Inorg. Chem.* **2014,** *53*, 7214-7226. (b) Tao, C.; Yu, Y.; Wei-Wei, L.; Wen-Bing, Q.; Ting-Bin, W., Efficient endo Cycloisomerization of Terminal Alkynols Catalyzed by a New Ruthenium Complex with 8-(Diphenylphosphino)quinoline Ligand and Mechanistic Investigation. *Chem. – Eur. J.* **2018,** *24*, 1606-1618

[29] Tsukuda, T.; Nishigata, C.; Arai, K.; Tsubomura, T., Photophysical properties of copper(I) and zinc(II) complexes containing phosphinoquinoline ligands. *Polyhedron* **2009,** *28*, 7-12.

[30] Suzuki, T.; Kotera, M.; Takayama, A.; Kojima, M., Crystal structures of (azido)(pentamethylcyclopentadienyl)iridium(III) complexes containing various types of bidentate ligands. *Polyhedron* **2009,** *28*, 2287-2293.

[31] Kittaneh, I. M.; Hodali, H. A.; Tayim, H. A., Complexes of some mixed-donor ligands with Rh(I), Ir(I) and Ir(III). *Inorg. Chim. Acta.* **1982,** *60*, 223-226.

[32] White, C.; Yates, A.; Maitlis, P. M., (η^5-Pentamethylcyclopentadienyl) Rhodium and -Iridium Compounds. *Inorg. Synth.* **1992,** *29*, 228-234

[33] Nutton, A.; Bailey, P. M.; Maitlis, P. M. Pentamethylcyclopentadienylrhodium and -iridium complexes. Part 29. Syntheses and x-ray structure determinations of tri-micro -hydroxybis[(h-pentamethylcyclopentadienyl)rhodium] hydroxide undecahydrate and -iridium acetate tetradecahydrate and related complexes. *J. Chem. Soc., Dalton Trans.* **1981**, 1997-2002.

[34] Issleib, K.; Haftendorn, M., Alkali Phosphorus Compounds and Their Reactive Behavior .43. 8-Quinolylphosphines. *Z. Anorg. Allg. Chem.* **1970,** *376*, 79-86

[35] Feltham, R. D.; Metzger, H. G., Synthesis of Vicinal Bis(Dimethylarsino) Compounds. *J. Organomet. Chem.* **1971,** *33*, 347-86

[36] Dadci, L.; Elias, H.; Frey, U.; Hornig, A.; Koelle, U.; Merbach, A. E.; Paulus, H.; Schneider, J. S., Pi-Arene Aqua Complexes of Cobalt, Rhodium, Iridium, and Ruthenium - Preparation, Structure, and Kinetics of Water Exchange and Water Substitution. *Inorg. Chem.* **1995,** *34*, 306-315

[37] Saveant, J.-M., *Elements of Molecular and Biomolecular Electrochemistry*. Wiley: Hoboken, NJ, 2006.

[38] (a) Blakemore, J. D.; Hernandez, E. S.; Sattler, W.; Hunter, B. M.; Henling, L. M.; Brunschwig, B. S.; Gray, H. B., Pentamethylcyclopentadienyl rhodium complexes. *Polyhedron* **2014,** *84*, 14-18. (b) Nakai, H.; Jeong, K.; Matsumoto, T.; Ogo, S., Catalytic C-F Bond Hydrogenolysis of Fluoroaromatics by [(η5-C5Me5)RhI(2,2'-bipyridine)]. *Organometallics* **2014,** *33*, 4349-4352.

[39] Johnson, S. I.; Gray, H. B.; Blakemore, J. D.; Goddard, W. A., Role of Ligand Protonation in Dihydrogen Evolution from a Pentamethylcyclopentadienyl Rhodium Catalyst. *Inorg. Chem.* **2017,** *56*, 11375-11386.

[40] Kaim, W.; Reinhardt, R.; Waldhor, E.; Fiedler, J., Electron transfer and chloride ligand dissociation in complexes [(C(5)Me(5))ClM(bpy)](+)/[(C(5)Me(5))M(bpy)](n) (M=Co, Rh, Ir; n=2+,+,0,-): A combined electrochemical and spectroscopic investigation. *J. Organomet. Chem.* **1996,** *524*, 195-202

[41] Chardon-Noblat, S.; Cosnier, S.; Deronzier, A.; Vlachopoulos, N., Electrochemical Properties of [(C5me5)Rhiii(L)Cl]+ Complexes (L=2,2'-Bipyridine or 1,10-Phenanthroline Derivatives) in Solution and in Related Polypyrrolic Films - Application to Electrocatalytic Hydrogen Generation. *J. Electroanal. Chem.* **1993,** *352*, 213-228

[42] (a) White, C.; Thompson, S. J.; Maitlis, P. M., Pentamethylcyclopentadienyl-rhodium and -iridium complexes. Part XII. Tris(solvent) complexes and complexes of [small eta]6-benzene, -naphthalene, -phenanthrene, -indene, -indole, and -fluorene and [small eta]5-lndenyl and -indolyl. *J. Chem. Soc., Dalton Trans.* **1977,** 1654-1661. (b) Blakemore, J. D.; Schley, N. D.; Balcells, D.; Hull, J. F.; Olack, G. W.; Incarvito, C. D.; Eisenstein, O.; Brudvig, G. W.; Crabtree, R. H., Half-Sandwich Iridium Complexes for Homogeneous Water-Oxidation Catalysis. *J. Am. Chem. Soc.* **2010,** *132*, 16017-16029.

[43] Connelly, N. G.; Geiger, W. E., Chemical Redox Agents for Organometallic Chemistry. *Chem. Rev.* **1996,** *96*, 877-910.

[44] (a) By comparison, reduction of bpy-supported [Cp*Rh] complexes results in notable changes in the C–C bond lengths of the ligand scaffold (best observed in the contraction of the interpyridine C–C bond), as determined by single-crystal XRD. These observations have been taken as evidence of substantial delocalization of electron

density into the π-system of the aromatic ligand. (b) Gore-Randall, E.; Irwin, M.; Denning, M. S.; Goicoechea, J. M., Synthesis and Characterization of Alkali-Metal Salts of 2,2′- and 2,4′-Bipyridyl Radicals and Dianions. *Inorg. Chem.* **2009,** *48*, 8304-8316.

[45] Bard, A. J.; Faulkner, L. R., *Electrochemistry: Fundamentals and Applications*. 2nd ed.; John Wiley and Sons Inc.: Hoboken, 2001.

[46] Lever, A. B. P., Electrochemical parametrization of metal complex redox potentials, using the ruthenium(III)/ruthenium(II) couple to generate a ligand electrochemical series. *Inorg. Chem.* **1990,** *29*, 1271-1285.

[47] Muckerman, J. T.; Skone, J. H.; Ning, M.; Wasada-Tsutsui, Y., Toward the accurate calculation of pKa values in water and acetonitrile. *Biochim. Biophys. Acta Bioenerg.* **2013,** *1827*, 882-891.

[48] (a) The data provide an estimated Rh–H41 distance of 1.48(4) Å. However, the large amount of electron density associated with the rhodium center could lead to underestimation of this bond distance. See the following reference for more information: (b) Schmidtmann, M.; Coster, P.; Henry, P. F.; Ting, V. P.; Weller, M. T.; Wilson, C. C., Determining hydrogen positions in crystal engineered organic molecular complexes by joint neutron powder and single crystal X-ray diffraction. *CrystEngComm* **2014,** *16*, 1232-1236.

[49] Appel, A. M.; Helm, M. L., Determining the Overpotential for a Molecular Electrocatalyst. *ACS Catal.* **2014,** *4*, 630-633.

[50] Creutz, C., Bipyridine radical ions. *Comments Inorg. Chem.* **1982,** *1*, 293-311.

[51] To report the ratio of enhancement, the peak current density associated with the reduction of **1-Cl** to **2** was divided by two to account for the two-electron nature of the wave.

[52] Fulmer, G. R.; Miller, A. J. M.; Sherden, N. H.; Gottlieb, H. E.; Nudelman, A.; Stoltz, B. M.; Bercaw, J. E.; Goldberg, K. I., NMR Chemical Shifts of Trace Impurities: Common Laboratory Solvents, Organics, and Gases in Deuterated Solvents Relevant to the Organometallic Chemist. *Organometallics* **2010,** *29*, 2176-2179.

[53] Harris, R. K.; Becker, E. D.; Cabral De Menezes, S. M.; Goodfellow, R.; Granger, P., NMR nomenclature. Nuclear spin properties and conventions for chemical shifts (IUPAC recommendations 2001). *Pure Appl. Chem.* **2001,** *73*, 1795-1818.

[54] Harris, R. K.; Becker, E. D.; Cabral De Menezes, S. M.; Granger, P.; Hoffman, R. E.; Zilm, K. W., Further conventions for NMR shielding and chemical shifts: (IUPAC recommendations 2008). *Pure Appl. Chem.* **2008,** *80*, 59-84.